

Improving the Top EFT Fit with Boosted Reconstruction Techniques

L. Moore¹, based on (1607.04304) with C. Englert¹, K. Nordström¹.
& M. Russell¹

¹Particle Physics Theory
University of Glasgow

LHC Top Working Group
EFT Session

- 1 Recap - $t\bar{t}$ EFT
- 2 Constraining EFT in $t\bar{t}$ Production
- 3 Analysis Strategy
- 4 Results
- 5 Summary and Conclusions

- Absence of evidence for BSM states in $t\bar{t}$ resonance searches
 $\implies \Lambda_{\text{NP}} \gg v$: low-energy signature of New Physics in the top sector should be well-described by the SMEFT
- Leading non-resonant effects in top physics arise from dimension-six operators with unknown couplings \implies use measurements to constrain Wilson Coefficients $C_i/\Lambda_{\text{NP}}^2$
- EFT operators' influence most pronounced at large momentum transfers $d\sigma_{\text{D6}} \propto \frac{p_T^2}{\Lambda_{\text{NP}}^2} \implies$ high top $p_T \iff$ NP enhanced
- Extracting information from sensitive region of phase space requires $t\bar{t}$ reconstruction at 13 TeV (and beyond)

- Absence of evidence for BSM states in $t\bar{t}$ resonance searches $\implies \Lambda_{\text{NP}} \gg v$: low-energy signature of New Physics in the top sector should be well-described by the SMEFT
- Leading non-resonant effects in top physics arise from dimension-six operators with unknown couplings \implies use measurements to constrain Wilson Coefficients $C_i/\Lambda_{\text{NP}}^2$
- EFT operators' influence most pronounced at large momentum transfers $d\sigma_{\text{D6}} \propto \frac{p_T^2}{\Lambda_{\text{NP}}^2} \implies$ high top $p_T \iff$ NP enhanced
- Extracting information from sensitive region of phase space requires $t\bar{t}$ reconstruction at 13 TeV (and beyond)

- Absence of evidence for BSM states in $t\bar{t}$ resonance searches $\implies \Lambda_{\text{NP}} \gg v$: low-energy signature of New Physics in the top sector should be well-described by the SMEFT
- Leading non-resonant effects in top physics arise from dimension-six operators with unknown couplings \implies use measurements to constrain Wilson Coefficients $C_i/\Lambda_{\text{NP}}^2$
- EFT operators' influence most pronounced at large momentum transfers $d\sigma_{\text{D6}} \propto \frac{p_T^2}{\Lambda_{\text{NP}}^2} \implies$ high top $p_T \iff$ NP enhanced
- Extracting information from sensitive region of phase space requires $t\bar{t}$ reconstruction at 13 TeV (and beyond)

- Absence of evidence for BSM states in $t\bar{t}$ resonance searches $\implies \Lambda_{\text{NP}} \gg v$: low-energy signature of New Physics in the top sector should be well-described by the SMEFT
- Leading non-resonant effects in top physics arise from dimension-six operators with unknown couplings \implies use measurements to constrain Wilson Coefficients $C_i/\Lambda_{\text{NP}}^2$
- EFT operators' influence most pronounced at large momentum transfers $d\sigma_{\text{D6}} \propto \frac{p_T^2}{\Lambda_{\text{NP}}^2} \implies$ high top $p_T \iff$ NP enhanced
- Extracting information from sensitive region of phase space requires $t\bar{t}$ reconstruction at 13 TeV (and beyond)

Objective:

Quantify scope for strengthening current constraints by applying **jet substructure algorithms** to efficiently reconstruct boosted tops.

EFT 101

$$\mathcal{L}_{\text{BSM}}(\{\Phi_{\text{SM}}\}, \{\mathcal{X}_{\text{NP}}\}) \rightarrow \mathcal{L}_{\text{SM}}(\{\Phi_{\text{SM}}\}) + \frac{C_i}{\Lambda^2} \mathcal{O}_i(\{\Phi_{\text{SM}}\}) + \dots$$

UV Completion \rightarrow Standard Model + Dimension Six Operators

- In the regime $q^2 < m_{\mathcal{X}}^2$, heavy states interacting with SM degrees of freedom **decouple**, generating a set of local operators \mathcal{O}_i .
- The short-distance structure of the theory determines the values of the effective coupling constants $\frac{C_i}{\Lambda^2} = \frac{f(g_{\mathcal{X}})}{m_{\mathcal{X}}^2}$
- Gauge invariance + B -conservation identifies **59 independent operators** \mathcal{O}_i at dimension-six (**Grzadkowski et al. 1008.4884**)
- The leading modifications to observables arise from the interference of SM matrix elements with those mediated by \mathcal{O}_i ;

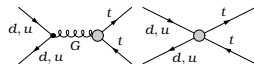
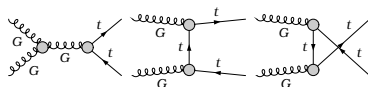
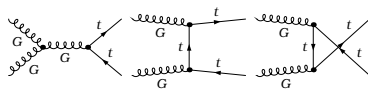
$$d\sigma_{\text{D6}} \propto \frac{C_i}{\Lambda^2} \int d\Pi \Re(\mathcal{M}_{\text{SM}}^* \mathcal{M}_{\text{D6}}) + \mathcal{O}(\Lambda^{-4}) = \frac{q^2}{\Lambda^2} \times (\dots)$$



$t\bar{t}$ Production in the SMEFT

Coefficient C_i	Operator \mathcal{O}_i
C_G	$f_{ABC} G_\mu^{A\nu} G_\nu^{B\lambda} G_\lambda^{C\mu}$
C_{uG}^{33}	$(\bar{q}\sigma^{\mu\nu} T^A u)\tilde{\varphi} G_{\mu\nu}^A$
$C_{qq}^{(1)}$	$(\bar{q}\gamma_\mu q)(\bar{q}\gamma^\mu q)$
$C_{qq}^{(3)}$	$(\bar{q}\gamma_\mu \tau^I q)(\bar{q}\gamma^\mu \tau^I q)$
C_{uu}	$(\bar{u}\gamma_\mu u)(\bar{u}\gamma^\mu u)$
$C_{qu}^{(8)}$	$(\bar{q}\gamma_\mu T^A q)(\bar{u}\gamma^\mu T^A u)$
$C_{qd}^{(8)}$	$(\bar{q}\gamma_\mu T^A q)(\bar{d}\gamma^\mu T^A d)$
$C_{ud}^{(8)}$	$(\bar{u}\gamma_\mu T^A u)(\bar{d}\gamma^\mu T^A d)$

Table : D6 operators in $t\bar{t}$ production. ψ^4 operators interfere in four linear combinations $C_{u,d}^{1,2}$.



$t\bar{t}$ Production in the SMEFT

Coefficient C_i	Operator \mathcal{O}_i
C_G	$f_{ABC} G_\mu^{A\nu} G_\nu^{B\lambda} G_\lambda^{C\mu}$
C_{uG}^{33}	$(\bar{q}\sigma^{\mu\nu} T^A u)\tilde{\phi} G_{\mu\nu}^A$
$C_{qq}^{(1)}$	$(\bar{q}\gamma_\mu q)(\bar{q}\gamma^\mu q)$
$C_{qq}^{(3)}$	$(\bar{q}\gamma_\mu \tau^I q)(\bar{q}\gamma^\mu \tau^I q)$
C_{uu}	$(\bar{u}\gamma_\mu u)(\bar{u}\gamma^\mu u)$
$C_{qu}^{(8)}$	$(\bar{q}\gamma_\mu T^A q)(\bar{u}\gamma^\mu T^A u)$
$C_{qd}^{(8)}$	$(\bar{q}\gamma_\mu T^A q)(\bar{d}\gamma^\mu T^A d)$
$C_{ud}^{(8)}$	$(\bar{u}\gamma_\mu T^A u)(\bar{d}\gamma^\mu T^A d)$

Table : Leading D6 operators in $t\bar{t}$ production and some possible UV origins.

Broad coverage of candidate UV-complete models:

- Heavy coloured fermions, technihadrons, gluon substructure . . . **(Cho et al. 9307345)**
- Composite top scenarios **(Englert et al. 1401.1502)**
- W' & Z' s **(Buckley et al. 1512.03360)**
- Heavy axigluons **(Cvetic et al. 1209.2741)**

An (Abridged) Brief History of t -EFT

- SMEFT $t\bar{t}$ phenomenology initially explored in e.g. **(Zhang et al. 1008.3869, Degrande et al. 1010.6304)** and more . . .
- Steadily accumulating, limited NLO SMEFT predictions in top physics, in e.g. t -decay **(Zhang 1404.1264)**, $t\bar{t}$ **(Franzosi et al. 1503.08841)**, single top **(Zhang 1601.06163)**, $t\bar{t}V$ **((Bylund et al. 1601.08193))**, $t\bar{t}H$ **(Maltoni et al. 1607.05330)** . . .
- Global C_i constraints available; PEWM operators **(Zhang et al. 1201.6670)** & **(de Blas et al. 1507.00757)**, FCNC operators **(Durieux et al. 1412.7166)**, $t\bar{t}$ + single top & more **(Buckley et al. 1506.08845, 1512.03360)** . . .
- Boosted $t\bar{t}$ investigations; A_C @ high $\beta_{t\bar{t}}$ **(Aguilar-Saavedra et al. 1109.3710)**, \mathcal{O}_{uG}^{33} @ high $m_{t\bar{t}}$ **(Aguilar-Saavedra et al. 1412.6654v2)**, composite top operators (HEPTOPTAGGER) **(Englert et al. 1401.1502v1)** . . .

TOPFITTER Constraints on $t\bar{t}$ Operators

- Fit MC to parton-level unfolded inclusive + differential top measurements
- Current global limits on C_i/Λ^2 extracted predominantly from Run I datasets utilizing resolved analyses
- Weak limits on C_i/Λ^2 inherently limit utility of EFT expansion: NP decoupled $\implies \Lambda > m_{t\bar{t}}^{\max}$
- Strengthening constraints \implies extend range of validity of EFT

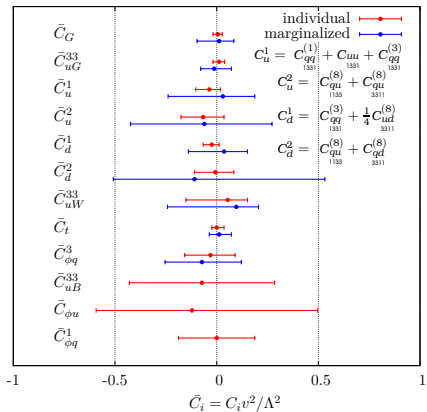


Figure : (TOPFITTER 95% CL (Buckley et al. 1512.03360))

Improving Constraints in $t\bar{t}$ Production

- Capitalizing on higher \mathcal{L} & \sqrt{s} in Run II (and beyond) will require extracting information from boosted tops
- NP-sensitive phase space region subject to larger uncertainties; lower statistics, larger theory uncertainty. . .
- Top reconstruction at high p_T qualitatively different - jet substructure techniques necessary

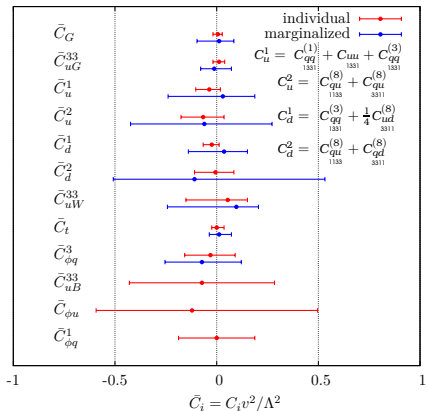


Figure : (TOPFITTER 95% CL (Buckley et al. 1512.03360))

Improving Constraints in $t\bar{t}$ Production

- Capitalizing on higher \mathcal{L} & \sqrt{s} in Run II (and beyond) will require extracting information from boosted tops
- NP-sensitive phase space region subject to larger uncertainties; lower statistics, larger theory uncertainty. . .
- Top reconstruction at high p_T qualitatively different - jet substructure techniques necessary

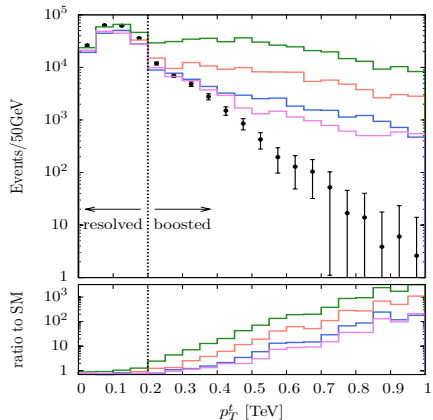


Figure : p_T^t spectrum @ 30 fb^{-1} ,
 $C_u^1 = C_u^2 = C_d^1 = C_d^2 = 10 \text{ TeV}^{-2}$

Improving Constraints in $t\bar{t}$ Production

- Capitalizing on higher \mathcal{L} & \sqrt{s} in Run II (and beyond) will require extracting information from boosted tops
- NP-sensitive phase space region subject to larger uncertainties; lower statistics, larger theory uncertainty. . .
- Top reconstruction at high p_T qualitatively different - jet substructure techniques necessary

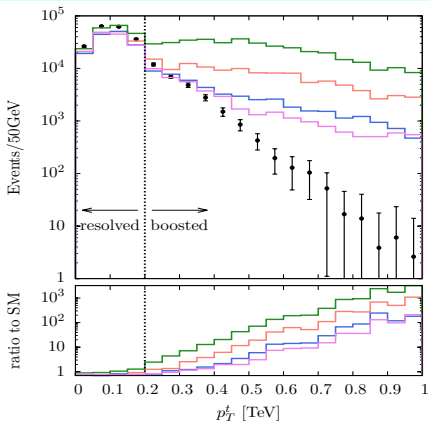


Figure : p_T^t spectrum @ 30 fb^{-1} ,
 $C_u^1 = C_u^2 = C_d^1 = C_d^2 = 10 \text{ TeV}^{-2}$

Boosted vs. Resolved Top Kinematics



Figure : Resolved & Boosted topologies. Credit: **(CMS @ Universität Hamburg)**

$$d_{j_1 j_2} = \frac{\Delta R_{j_1 j_2}^2}{R_{\text{jet}}^2} \min(p_{T j_1}^{2n}, p_{T j_2}^{2n}), \quad n = \{1 (k_T), 0 (C/A), -1 (\text{anti-}k_T)\}.$$

$$\Delta R \equiv \sqrt{\Delta\phi^2 + \Delta\eta^2}$$

- $\Delta R_{bjj} > R_{\text{jet}}$
- Isolated jets \leftrightarrow hard partons
- Individually characterized by QCD \rightarrow reconstruct traditional jets
- $\Delta R_{bjj} \sim R_{\text{jet}}$
- Merged 'fat' jets
- Individually QCD + massive decays \rightarrow **boosted top-tagging**

Boosted vs. Resolved Top Kinematics



Figure : Resolved & Boosted topologies. Credit: **(CMS @ Universität Hamburg)**

- Boosted and resolved tops \leftrightarrow distinct systematic uncertainties.

$$\sigma_{p_T^t > 200 \text{ GeV}}^{t\bar{t}} / \sigma_{\text{tot}}^{t\bar{t}} \sim 10\% \text{ @ } 13 \text{ TeV} - \text{data-starved @ high } p_T$$

- How does the relative weight of high p_T tops in constraining C_i/Λ^2 change with increasing \mathcal{L}_{int} over the lifetime of the LHC, and as a function of experimental systematics and theory uncertainties?

Boosted vs. Resolved Top Kinematics



Figure : Resolved & Boosted topologies. Credit: **(CMS @ Universität Hamburg)**

- Boosted and resolved tops \leftrightarrow distinct systematic uncertainties.

$$\sigma_{p_T^t > 200 \text{ GeV}}^{t\bar{t}} / \sigma_{\text{tot}}^{t\bar{t}} \sim 10\% \text{ @ } 13 \text{ TeV} - \text{data-starved @ high } p_T$$

- How does the relative weight of high p_T tops in constraining C_i/Λ^2 change with increasing \mathcal{L}_{int} over the lifetime of the LHC, and as a function of **experimental systematics** and **theory uncertainties**?

Boosted vs. Resolved Top Kinematics



Figure : Resolved & Boosted topologies. Credit: **(CMS @ Universität Hamburg)**

- Boosted and resolved tops \leftrightarrow distinct systematic uncertainties.
 $\sigma_{p_T^t > 200 \text{ GeV}}^{t\bar{t}} / \sigma_{\text{tot}}^{t\bar{t}} \sim 10\% @ 13 \text{ TeV}$ - data-starved @ high p_T
- How does the relative weight of high p_T tops in constraining C_i/Λ^2 change with increasing \mathcal{L}_{int} over the lifetime of the LHC, and as a function of **experimental systematics** and **theory uncertainties**?

Can investigate interplay of these factors by partitioning phase space by p_T^t and performing complementary resolved and boosted analyses on representative hadron-level pseudodata samples

Setup - Theory Samples (I)

- We implemented the ‘Warsaw’ Basis (**Grzadkowski et al. 1008.4884**) in FEYNRULES (**Alloul et al. 1310.1921**), interfaced via UFO (**Degrande et al. 1108.2040**) to MG5_AMC (**Alwall et al. 1405.0301**) → parton-level $t\bar{t}$ events @ LO in SMEFT
- Reweight distributions to NLO QCD binwise with SM K-factors, obtained from MCFM (**Campbell et al. 1007.3492**) & cross-checked with with MC@NLO (**Alwall et al. 1405.0301**)
- Theory uncertainties: scales varied independently between $m_t/2 < \mu_{R,F} < 2m_t$. PDF uncertainties estimated by generating samples with CT14 (**Dulat et al. 1506.07443**), MMHT14 (**Harland-Lang et al. 1412.3989**) and NNPDF3.0 (**Ball et al. 1410.8849**) PDFs as per PDF4LHC WG recommendations for Run II (**Butterworth et al. 1510.03865**). Full scale + PDF envelope defines theory band. Treated as uncorrelated with $\epsilon_{\text{sys}}^{\text{exp}}$ & fixed with \mathcal{L} .

Setup - Theory Samples (I)

- We implemented the ‘Warsaw’ Basis (**Grzadkowski et al. 1008.4884**) in FEYNRULES (**Alloul et al. 1310.1921**), interfaced via UFO (**DeGrande et al. 1108.2040**) to MG5_AMC (**Alwall et al. 1405.0301**) → parton-level $t\bar{t}$ events @ LO in SMEFT
- Reweight distributions to NLO QCD binwise with SM K-factors, obtained from MCFM (**Campbell et al. 1007.3492**) & cross-checked with with MC@NLO (**Alwall et al. 1405.0301**)
- Theory uncertainties: scales varied independently between $m_t/2 < \mu_{R,F} < 2m_t$. PDF uncertainties estimated by generating samples with CT14 (**Dulat et al. 1506.07443**), MMHT14 (**Harland-Lang et al. 1412.3989**) and NNPDF3.0 (**Ball et al. 1410.8849**) PDFs as per PDF4LHC WG recommendations for Run II (**Butterworth et al. 1510.03865**). Full scale + PDF envelope defines theory band. Treated as uncorrelated with $\epsilon_{\text{sys}}^{\text{exp}}$ & fixed with \mathcal{L} .

Setup - Theory Samples (I)

- We implemented the ‘Warsaw’ Basis (**Grzadkowski et al. 1008.4884**) in FEYNRULES (**Alloul et al. 1310.1921**), interfaced via UFO (**Degrande et al. 1108.2040**) to MG5_AMC (**Alwall et al. 1405.0301**) → parton-level $t\bar{t}$ events @ LO in SMEFT
- Reweight distributions to NLO QCD binwise with SM K-factors, obtained from MCFM (**Campbell et al. 1007.3492**) & cross-checked with with MC@NLO (**Alwall et al. 1405.0301**)
- Theory uncertainties: scales varied independently between $m_t/2 < \mu_{R,F} < 2m_t$. PDF uncertainties estimated by generating samples with CT14 (**Dulat et al. 1506.07443**), MMHT14 (**Harland-Lang et al. 1412.3989**) and NNPDF3.0 (**Ball et al. 1410.8849**) PDFs as per PDF4LHC WG recommendations for Run II (**Butterworth et al. 1510.03865**). Full scale + PDF envelope defines theory band. Treated as uncorrelated with $\epsilon_{\text{sys}}^{\text{exp}}$ & fixed with \mathcal{L} .

Setup - SMEFT Theory Samples (II)

- Construct a logarithmically **random-sampled parameter space** for C_i/Λ^2 centred about $\{C_i\} = 0$, and generate theory predictions and uncertainties as described at each point
- Fit an **interpolation-based parameterizing function** to supply predictions for arbitrary values of $\{C_i\}$ for each bin

Setup - SMEFT Theory Samples (II)

- Construct a logarithmically **random-sampled parameter space** for C_i/Λ^2 centred about $\{C_i\} = 0$, and generate theory predictions and uncertainties as described at each point
- Fit an **interpolation-based parameterizing function** to supply predictions for arbitrary values of $\{C_i\}$ for each bin

This takes the form of a fourth order polynomial in the coefficients $\{C_i\}$ for each bin b :

$$f_b(\{C_i\}) = \alpha_0^b + \sum_i \beta_i^b C_i + \sum_{i \leq j} \gamma_{ij}^b C_{ij} + \dots$$

Once f_b is constructed, all that remains is to define a χ^2 goodness of fit function between theory and (pseudo-)data, and minimise it to obtain exclusion contours for $\{C_i\}$.

Setup - SM Pseudodata Samples

- Simulate hadron-level $t\bar{t}$ events in the **semileptonic decay channel** by showering $\{C_i\} = 0$ point in HERWIG++ (**Bahr et al. 0803.0883**, **Bell et al. 1512.01178**)
- Extract event samples corresponding to representative LHC integrated luminosity scenarios $\mathcal{L}_{\text{int}} = \{30\text{fb}^{-1}, 300\text{fb}^{-1}, 3\text{ab}^{-1}\}$
- $p_T^t \geq 200\text{GeV}$ chosen as threshold above which an event qualifies for boosted reconstruction (based on top-tagging efficiency (**Plehn et al. 1112.4441**))
- Resolved and boosted analyses for each p_T^t region implemented in RIVET (**Buckley et al. 1003.0694**)

Setup - SM Pseudodata Samples

- Simulate hadron-level $t\bar{t}$ events in the **semileptonic decay channel** by showering $\{C_i\} = 0$ point in HERWIG++ (**Bahr et al. 0803.0883**, **Bell et al. 1512.01178**)
- Extract event samples corresponding to representative LHC integrated luminosity scenarios $\mathcal{L}_{\text{int}} = \{30\text{fb}^{-1}, 300\text{fb}^{-1}, 3\text{ab}^{-1}\}$
- $p_T^t \geq 200\text{GeV}$ chosen as threshold above which an event qualifies for boosted reconstruction (based on top-tagging efficiency (**Plehn et al. 1112.4441**))
- Resolved and boosted analyses for each p_T^t region implemented in RIVET (**Buckley et al. 1003.0694**)

Setup - SM Pseudodata Samples

- Simulate hadron-level $t\bar{t}$ events in the **semileptonic decay channel** by showering $\{C_i\} = 0$ point in HERWIG++ (**Bahr et al. 0803.0883**, **Bell et al. 1512.01178**)
- Extract event samples corresponding to representative LHC integrated luminosity scenarios $\mathcal{L}_{\text{int}} = \{30\text{fb}^{-1}, 300\text{fb}^{-1}, 3\text{ab}^{-1}\}$
- $p_T^t \geq 200\text{GeV}$ chosen as threshold above which an event qualifies for boosted reconstruction (based on top-tagging efficiency (**Plehn et al. 1112.4441**))
- Resolved and boosted analyses for each p_T^t region implemented in RIVET (**Buckley et al. 1003.0694**)

Setup - SM Pseudodata Samples

- Simulate hadron-level $t\bar{t}$ events in the **semileptonic decay channel** by showering $\{C_i\} = 0$ point in HERWIG++ (**Bahr et al. 0803.0883**, **Bell et al. 1512.01178**)
- Extract event samples corresponding to representative LHC integrated luminosity scenarios $\mathcal{L}_{\text{int}} = \{30\text{fb}^{-1}, 300\text{fb}^{-1}, 3\text{ab}^{-1}\}$
- $p_T^t \geq 200\text{GeV}$ chosen as threshold above which an event qualifies for boosted reconstruction (based on top-tagging efficiency (**Plehn et al. 1112.4441**))
- Resolved and boosted analyses for each p_T^t region implemented in RIVET (**Buckley et al. 1003.0694**)

Analysis Strategy

- We require a **single charged lepton with $p_T > 30\text{GeV}$** , and missing transverse energy vector with magnitude **$E_T^{\text{miss}} > 30\text{GeV}$** . The leptonic W -boson is reconstructed from these by assuming it was produced on-shell. We do not consider the τ decay mode
- Jets are then clustered using the anti- k_T algorithm (**Cacciari et al. 0802.1189**) using FASTJET (**Cacciari et al. 1111.6097**) in two separate groups with $R = (0.4, 1.2)$ requiring **$p_T > (30, 200)\text{GeV}$** respectively, and jets which overlap with the charged lepton are removed.
- The **$R = 1.2$ fat jets** are required to be **within $|\eta| < 2$** , and the $R = 0.4$ small jets are b-tagged within the same η range with an efficiency of 70% and fake rate of 1%

Analysis Strategy

- We require a **single charged lepton with $p_T > 30\text{GeV}$** , and missing transverse energy vector with magnitude **$E_T^{\text{miss}} > 30\text{GeV}$** . The leptonic W -boson is reconstructed from these by assuming it was produced on-shell. We do not consider the τ decay mode
- Jets are then clustered using the anti- k_T algorithm (**Cacciari et al. 0802.1189**) using FASTJET (**Cacciari et al. 1111.6097**) in two separate groups with **$R = (0.4, 1.2)$** requiring **$p_T > (30, 200)\text{GeV}$** respectively, and jets which overlap with the charged lepton are removed.
- The **$R = 1.2$ fat jets** are required to be **within $|\eta| < 2$** , and the **$R = 0.4$ small jets** are b-tagged within the same η range with an efficiency of 70% and fake rate of 1%

Analysis Strategy

- We require a **single charged lepton with $p_T > 30\text{GeV}$** , and missing transverse energy vector with magnitude **$E_T^{\text{miss}} > 30\text{GeV}$** . The leptonic W -boson is reconstructed from these by assuming it was produced on-shell. We do not consider the τ decay mode
- Jets are then clustered using the anti- k_T algorithm (**Cacciari et al. 0802.1189**) using FASTJET (**Cacciari et al. 1111.6097**) in two separate groups with **$R = (0.4, 1.2)$** requiring **$p_T > (30, 200)\text{GeV}$** respectively, and jets which overlap with the charged lepton are removed.
- The **$R = 1.2$ fat jets** are required to be **within $|\eta| < 2$** , and the $R = 0.4$ small jets are b-tagged within the same η range with an efficiency of 70% and fake rate of 1%

Analysis Strategy - Boosted

If $n_{\text{fat}} \geq 1$ and $n_{\text{b-tagged}} \geq 1 \implies$ **boosted top-tag** of the leading fat jet using **HEPTopTAgGER (Plehn et al. 1006.2833, Kasieczka et al. 1503.05921)** and reconstruct t_{lept} using the leading, non-overlapping b-tagged small jet and the reconstructed leptonic W.

$$m_{\text{subjet}}^{\text{max}} = 30\text{GeV}$$

$$\mu_{\text{drop}} = 0.8$$

$$R_{\text{filt}} = 0.3$$

$$n_{\text{filt}} = 5$$

$$p_{T \text{ subjet}}^{\text{min}} = 30\text{GeV}$$

$$f_W = 15\%$$

$$150\text{GeV} < m_t^{\text{rec}} < 200\text{GeV}$$

Table : HEPTopTAgGER setup

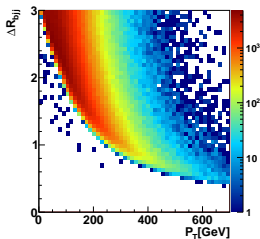


Figure : $\Delta R_{b_{ij}}^{\text{SM}}(p_T^t)$ (1112.4441 Plehn et al.)



Analysis Strategy - Resolved

- If no satisfactory fat jet exists \implies **require**
 $n_{\text{b-tagged}} \geq 2$ and $n_{\text{light}} \geq 2$
- Reconstruct hadronic W -boson by finding the light small jet pair that best reconstructs the W mass
- Reconstruct top candidates by similarly finding the pairs of reconstructed W -boson and b-tagged small jet that best reconstruct the top mass

Analysis Strategy - Resolved

- If no satisfactory fat jet exists \implies **require**
 $n_{\text{b-tagged}} \geq 2$ and $n_{\text{light}} \geq 2$
- Reconstruct hadronic W -boson by finding the light small jet pair that best reconstructs the W mass
- Reconstruct top candidates by similarly finding the pairs of reconstructed W -boson and b-tagged small jet that best reconstruct the top mass

Analysis Strategy - Resolved

- If no satisfactory fat jet exists \implies **require**
 $n_{\text{b-tagged}} \geq 2$ and $n_{\text{light}} \geq 2$
- Reconstruct hadronic W -boson by finding the light small jet pair that best reconstructs the W mass
- Reconstruct top candidates by similarly finding the pairs of reconstructed W -boson and b-tagged small jet that best reconstruct the top mass

Finally, regardless of the approach used, we require both top candidates to have $|m_{\text{cand}} - m_{\text{top}}| < 40\text{GeV}$. If this requirement is fulfilled the event passes the analysis.

Analysis Summary

<i>Leptons</i>	$p_T > 30 \text{ GeV}$ $ \eta < 4.2$
<i>Missing energy</i>	$E_T^{\text{miss}} > 30 \text{ GeV}$
<i>Small jets</i>	anti- k_T $R = 0.4$ $p_T > 30 \text{ GeV}, \eta < 2$
<i>Fat jets</i>	anti- k_T $R = 1.2$ $p_T > 200 \text{ GeV}, \eta < 2$
Resolved	≥ 4 jets w/ ≥ 2 b-tags
Boosted	≥ 1 fat jet, ≥ 1 w/ b-tag

Table : Summary of Rivet event selection criteria

- We chose the benchmark scenarios
 $\mathcal{L}_{\text{int}} = \{30, 300, 3000\} \text{ fb}^{-1}$
 with $\epsilon_{\text{syst}} = \{10\%, 20\%\}$
- Systematics inserted by defining a flat percentage interval associated with each bin
- Bounds presented here are 'one-at-a-time', i.e. not marginalised over the full operator set.

Analysis Summary

<i>Leptons</i>	$p_T > 30 \text{ GeV}$ $ \eta < 4.2$
<i>Missing energy</i>	$E_T^{\text{miss}} > 30 \text{ GeV}$
<i>Small jets</i>	anti- k_T $R = 0.4$ $p_T > 30 \text{ GeV}, \eta < 2$
<i>Fat jets</i>	anti- k_T $R = 1.2$ $p_T > 200 \text{ GeV}, \eta < 2$
Resolved	≥ 4 jets w/ ≥ 2 b-tags
Boosted	≥ 1 fat jet, ≥ 1 w/ b-tag

Table : Summary of Rivet event selection criteria

- We chose the benchmark scenarios
 $\mathcal{L}_{\text{int}} = \{30, 300, 3000\} \text{ fb}^{-1}$
 with $\epsilon_{\text{syst}} = \{10\%, 20\%\}$
- Systematics inserted by defining a flat percentage interval associated with each bin
- Bounds presented here are 'one-at-a-time', i.e. not marginalised over the full operator set.

Analysis Summary

<i>Leptons</i>	$p_T > 30 \text{ GeV}$ $ \eta < 4.2$
<i>Missing energy</i>	$E_T^{\text{miss}} > 30 \text{ GeV}$
<i>Small jets</i>	anti- k_T $R = 0.4$ $p_T > 30 \text{ GeV}, \eta < 2$
<i>Fat jets</i>	anti- k_T $R = 1.2$ $p_T > 200 \text{ GeV}, \eta < 2$
Resolved	≥ 4 jets w/ ≥ 2 b-tags
Boosted	≥ 1 fat jet, ≥ 1 w/ b-tag

Table : Summary of Rivet event selection criteria

- We chose the benchmark scenarios
 $\mathcal{L}_{\text{int}} = \{30, 300, 3000\} \text{ fb}^{-1}$
 with $\varepsilon_{\text{syst}} = \{10\%, 20\%\}$
- Systematics inserted by defining a flat percentage interval associated with each bin
- Bounds presented here are 'one-at-a-time', i.e. not marginalised over the full operator set.

95% C.L. @ $\mathcal{L}_{\text{int}} = 30 \text{ fb}^{-1}$, $\epsilon_{\text{sys}} = 20\%$

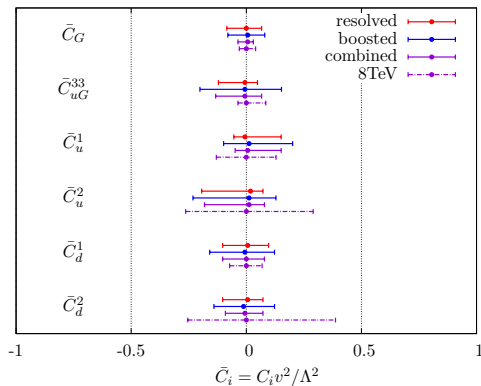


Figure : 1-dimensional 95% confidence intervals on C_i/Λ^2 for both selections using $\mathcal{L} = 30 \text{ fb}^{-1}$ and $\epsilon_{\text{sys}} = 20\%$, displayed together with TopFITTER constraints from unfolded 8 TeV p_T^t distributions.

Resolved - Relative Improvements w/ \mathcal{L}_{int} and ϵ_{sys}

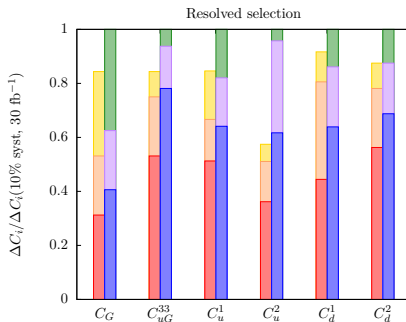


Figure : Fractional improvement on the 95% C.I., with each choice of ϵ_{sys} and \mathcal{L}_{int} , normalized to $\epsilon_{\text{sys}} = 20\%$ and $\mathcal{L}_{\text{int}} = 30\text{fb}^{-1}$.

$\{30\text{fb}^{-1}, 300\text{fb}^{-1}, 3\text{ab}^{-1}\}$ of data at at **20% systematics**.

$\{30\text{fb}^{-1}, 300\text{fb}^{-1}, 3\text{ab}^{-1}\}$ of data for **10% systematics**.

Resolved - Relative Improvements w/ \mathcal{L}_{int} and ϵ_{sys}

- We find that the limits on the coefficient C_G can be improved by 40% by going from 30 fb^{-1} to 300 fb^{-1} , and by a further 20% at 3 ab^{-1} .
- Systematics have a more modest effect: at 3 ab^{-1} limits marginally improved by 10% reduction. Improvements in the threshold region require collecting enough data to overcome the lack of sensitivity.

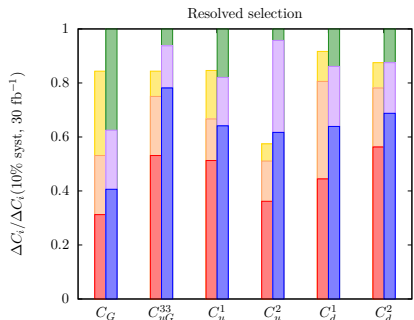


Figure : Relative 95% C.I., w/ $\{30, 300, 3000\} \text{ fb}^{-1}$ @ 20% systematics. $\{30, 300, 3000\} \text{ fb}^{-1}$ @ 10% systematics.

Resolved - Relative Improvements w/ \mathcal{L}_{int} and ϵ_{sys}

- We find that the limits on the coefficient C_G can be improved by 40% by going from 30 fb^{-1} to 300 fb^{-1} , and by a further 20% at 3 ab^{-1} .
- Systematics have a more modest effect:** at 3 ab^{-1} limits marginally improved by 10% reduction. Improvements in the threshold region require collecting enough data to overcome the lack of sensitivity.

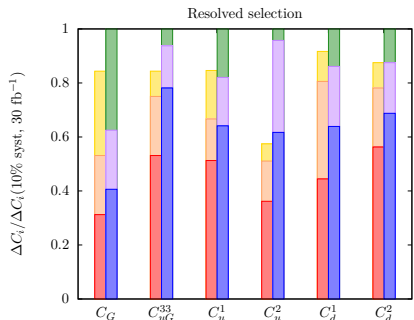


Figure : Relative 95% C.I., w/ $\{30, 300, 3000\} \text{ fb}^{-1}$ @ **20%** systematics. $\{30, 300, 3000\} \text{ fb}^{-1}$ @ **10%** systematics.

Resolved - Relative Improvements w/ \mathcal{L}_{int} and ϵ_{sys}

For the chromomagnetic dipole operator \mathcal{O}_{uG}^{33} , improving the experimental **systematics plays much more of a role**. A 10% improvement in systematics, coupled with an increase in statistics from 30 fb^{-1} to 300 fb^{-1} leads to stronger limits that maintaining current systematics and collecting a full 3 ab^{-1} of data.

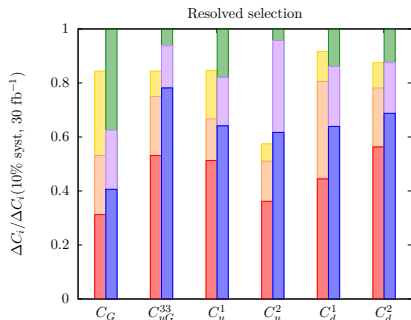


Figure : Relative 95% C.I., w/ $\{30, 300, 3000\} \text{ fb}^{-1}$ @ **20%** systematics. $\{30, 300, 3000\} \text{ fb}^{-1}$ @ **10%** systematics.

Resolved - Relative Improvements w/ \mathcal{L}_{int} and ϵ_{sys}

- Similar conclusions apply for the **four-quark operators**, to varying degrees, i.e. **reducing systematic uncertainties can provide comparable improvements** to collecting much larger data samples
- The Wilson coefficients C_1^u and C_2^u contributing to the $u\bar{u}$ channel **benefit more from reduced systematic uncertainties** than their $d\bar{d}$ counterparts

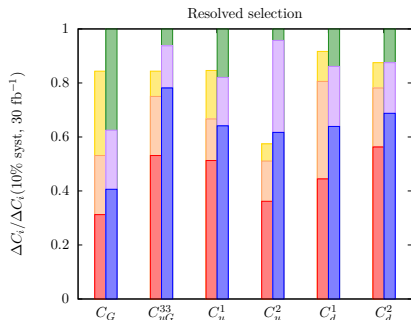


Figure : Relative 95% C.I., w/ $\{30, 300, 3000\} \text{fb}^{-1}$ @ **20%** systematics. $\{30, 300, 3000\} \text{fb}^{-1}$ @ **10%** systematics.

Resolved - Relative Improvements w/ \mathcal{L}_{int} and ϵ_{sys}

- Similar conclusions apply for the **four-quark operators**, to varying degrees, i.e. **reducing systematic uncertainties can provide comparable improvements** to collecting much larger data samples
- The Wilson coefficients C_1^u and C_2^u contributing to the $u\bar{u}$ channel **benefit more from reduced systematic uncertainties** than their $d\bar{d}$ counterparts

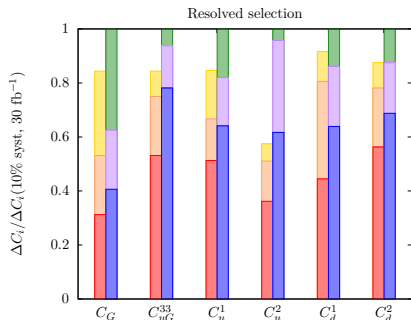


Figure : Relative 95% C.I., w/ $\{30, 300, 3000\} \text{fb}^{-1}$ @ **20%** systematics. $\{30, 300, 3000\} \text{fb}^{-1}$ @ **10%** systematics.

Boosted - Relative Improvements w/ \mathcal{L}_{int} and ϵ_{sys}

- In the boosted selection, **improving systematics** by 10% has **virtually no effect** on the improvement in the limits \implies statistics dominated @ 30 fb^{-1}
- For C_G , at 300 fb^{-1} some improvement can be made if systematics are reduced, beyond which systematics saturate the sensitivity to C_G , i.e. there is **no improvement to be made by collecting more data**.

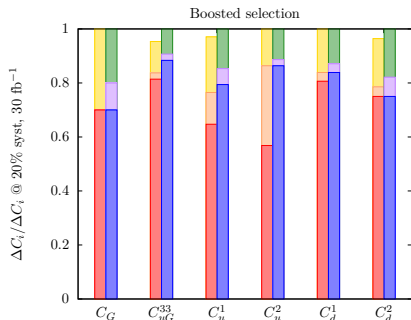


Figure : Relative 95% C.I., w/ $\{30, 300, 3000\} \text{ fb}^{-1}$ @ **20%** systematics. $\{30, 300, 3000\} \text{ fb}^{-1}$ @ **10%** systematics.

Boosted - Relative Improvements w/ \mathcal{L}_{int} and ϵ_{sys}

- In the boosted selection, **improving systematics** by 10% has **virtually no effect** on the improvement in the limits \implies statistics dominated @ 30 fb^{-1}
- For C_G , at 300 fb^{-1} some improvement can be made if systematics are reduced, beyond which systematics saturate the sensitivity to C_G , i.e. there is **no improvement to be made by collecting more data**.

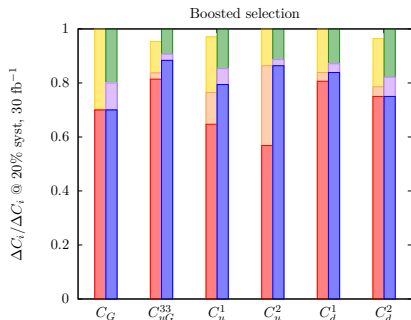


Figure : Relative 95% C.I., w/ $\{30, 300, 3000\} \text{ fb}^{-1}$ @ **20%** systematics. $\{30, 300, 3000\} \text{ fb}^{-1}$ @ **10%** systematics.

Boosted - Relative Improvements w/ \mathcal{L}_{int} and ϵ_{sys}

- For C_{uG}^{33} , a **modest improvement** can also be made both by reducing systematics by 10% and by increasing the dataset to 300 fb^{-1} . However, going beyond this, the improvement is minute.
- The **four-quark operators** again follow this trend, although C_u^1 and C_u^2 show much more of an improvement when going from 300 fb^{-1} to 3 ab^{-1} .

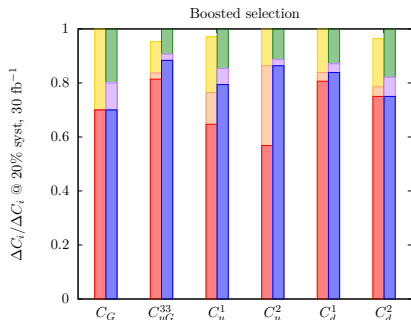


Figure : Relative 95% C.I., w/ $\{30, 300, 3000\} \text{ fb}^{-1}$ @ **20%** systematics. $\{30, 300, 3000\} \text{ fb}^{-1}$ @ **10%** systematics.

Boosted - Relative Improvements w/ \mathcal{L}_{int} and ϵ_{sys}

- For C_{uG}^{33} , a modest improvement can also be made both by reducing systematics by 10% and by increasing the dataset to 300 fb^{-1} . However, going beyond this, the improvement is minute.
- The four-quark operators again follow this trend, although C_u^1 and C_u^2 show much more of an improvement when going from 300 fb^{-1} to 3 ab^{-1} .

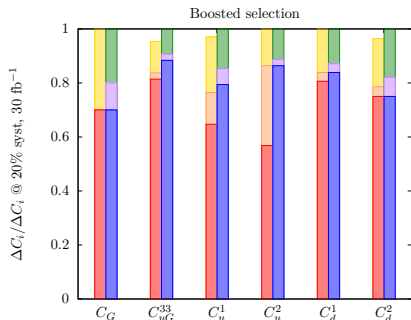


Figure : Relative 95% C.I., w/ $\{30, 300, 3000\} \text{ fb}^{-1}$ @ 20% systematics. $\{30, 300, 3000\} \text{ fb}^{-1}$ @ 10% systematics.

The Role of Theoretical Uncertainties (I)

- The scale and PDF variation procedure outlined typically leads to uncertainties in the **10-15% range**.
- Recently, **differential K -factors** for top pair production **at NNLO QCD** have become available, which have substantially reduced the scale uncertainties (**Czakon et al. 1601.05375, 1511.00549**). These are presently limited to the range $p_T^t < 400$ GeV, **applicable to the TeVatron and 8 TeV LHC**
- **NLO + RGE effects in EFT** important for measurements at LEP-level precision (**Berthier et al. 1508.05060**). At LHC, we find them to be **numerically insignificant** compared to the sources of uncertainty studied here.
- Not accounted for here is possibility of significant contribution from **interfering dimension-8 operators**

The Role of Theoretical Uncertainties (I)

- The scale and PDF variation procedure outlined typically leads to uncertainties in the **10-15% range**.
- Recently, **differential K -factors** for top pair production **at NNLO QCD** have become available, which have substantially reduced the scale uncertainties (**Czakon et al. 1601.05375, 1511.00549**). These are presently limited to the range $p_T^t < 400$ GeV, **applicable to the TeVatron and 8 TeV LHC**
- **NLO + RGE effects in EFT** important for measurements at LEP-level precision (**Berthier et al. 1508.05060**). At LHC, we find them to be **numerically insignificant** compared to the sources of uncertainty studied here.
- Not accounted for here is possibility of significant contribution from **interfering dimension-8 operators**

The Role of Theoretical Uncertainties (I)

- The scale and PDF variation procedure outlined typically leads to uncertainties in the **10-15% range**.
- Recently, **differential K -factors** for top pair production **at NNLO QCD** have become available, which have substantially reduced the scale uncertainties (**Czakon et al. 1601.05375, 1511.00549**). These are presently limited to the range $p_T^t < 400$ GeV, **applicable to the TeVatron and 8 TeV LHC**
- **NLO + RGE effects in EFT** important for measurements at LEP-level precision (**Berthier et al. 1508.05060**). At LHC, we find them to be **numerically insignificant** compared to the sources of uncertainty studied here.
- Not accounted for here is possibility of significant contribution from **interfering dimension-8 operators**

The Role of Theoretical Uncertainties (I)

- The scale and PDF variation procedure outlined typically leads to uncertainties in the **10-15% range**.
- Recently, **differential K -factors** for top pair production **at NNLO QCD** have become available, which have substantially reduced the scale uncertainties (**Czakon et al. 1601.05375, 1511.00549**). These are presently limited to the range $p_T^t < 400$ GeV, **applicable to the TeVatron and 8 TeV LHC**
- **NLO + RGE effects in EFT** important for measurements at LEP-level precision (**Berthier et al. 1508.05060**). At LHC, we find them to be **numerically insignificant** compared to the sources of uncertainty studied here.
- Not accounted for here is possibility of significant contribution from **interfering dimension-8 operators**

The Role of Theory Uncertainties (II)

Can get a feel for improvements given similar precision @ 13 TeV;

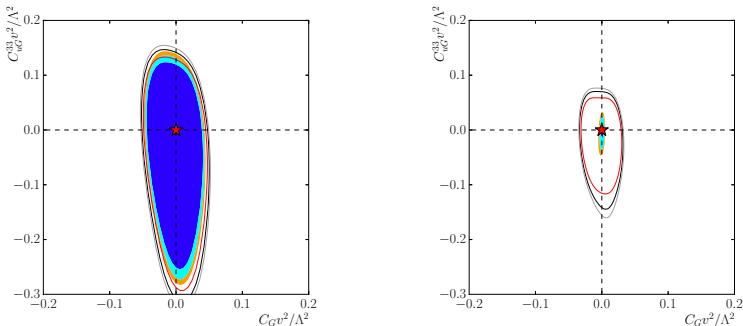


Figure : Left: 68%, 95% and 99% C.I. for C_G & C_{uG}^{33} , **Lines**: ($\epsilon_{\text{sys}} = 20\%$, $\mathcal{L}_{\text{int}} = 30 \text{ fb}^{-1}$) **with** NLO theoretical uncertainties. **Filled contours**: likewise, with **no** theoretical uncertainties. Right: Likewise, w/ ($\epsilon_{\text{sys}} = 10\%$, $\mathcal{L}_{\text{int}} = 3 \text{ ab}^{-1}$).

Consequences on EFT Validity

- Strength of constraints \iff range of EFT validity
- Match $\frac{C_i}{\Lambda^2} = \frac{g_*^2}{M_*^2}$
- Impose $M_* > m_{t\bar{t}}^{\max} = 2\text{TeV}$
- Weak constraint \implies larger g_* , higher-order corrections to BSM important
- Truncation at e.g. $\mathcal{O}(\Lambda^{-2})$ less reliable

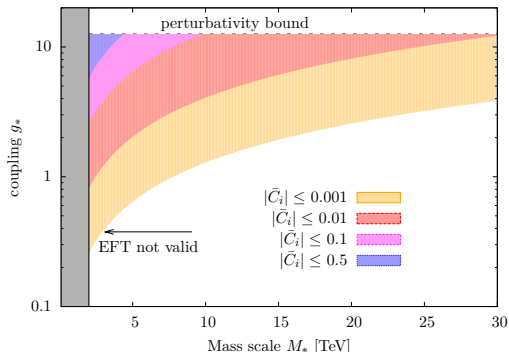


Figure : Areas in the $g_* - M_*$ plane. Coloured areas constrained in perturbative models subject to condition $C/\Lambda^2 = g_*^2/M_*^2$. Shaded grey area: mass scales $M_* < m_{t\bar{t}}^{\max}$

Consequences on EFT Validity

- Strength of constraints \iff range of EFT validity
- Match $\frac{C_i}{\Lambda^2} = \frac{g_*^2}{M_*^2}$
- Impose $M_* > m_{\tilde{t}\tilde{t}^*}^{\max} = 2\text{TeV}$
- Weak constraint \implies larger g_* , higher-order corrections to BSM important
- Truncation at e.g. $\mathcal{O}(\Lambda^{-2})$ less reliable

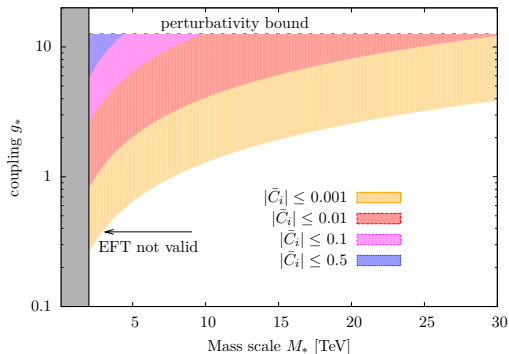


Figure : Areas in the $g_* - M_*$ plane. Coloured areas constrained in perturbative models subject to condition $C/\Lambda^2 = g_*^2/M_*^2$. Shaded grey area: mass scales $M_* < m_{\tilde{t}\tilde{t}^*}^{\max}$

Consequences on EFT Validity

- Strength of constraints
 \iff range of EFT
 validity
- Match $\frac{C_i}{\Lambda^2} = \frac{g_*^2}{M_*^2}$
- Impose
 $M_* > m_{\tilde{t}\tilde{t}}^{\max} = 2\text{TeV}$
- Weak constraint \implies
 larger g_* , higher-order
 corrections to BSM
 important
- Truncation at e.g.
 $\mathcal{O}(\Lambda^{-2})$ less reliable

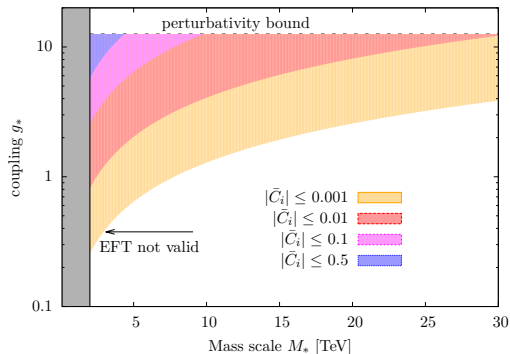


Figure : Areas in the $g_* - M_*$ plane. Coloured areas constrained in perturbative models subject to condition $C/\Lambda^2 = g_*^2/M_*^2$. Shaded grey area: mass scales $M_* < m_{\tilde{t}\tilde{t}}^{\max}$

Consequences on EFT Validity

- Strength of constraints \iff range of EFT validity
- Match $\frac{C_i}{\Lambda^2} = \frac{g_*^2}{M_*^2}$
- Impose $M_* > m_{t\bar{t}}^{\max} = 2\text{TeV}$
- Weak constraint \implies larger g_* , higher-order corrections to BSM important
- Truncation at e.g. $\mathcal{O}(\Lambda^{-2})$ less reliable

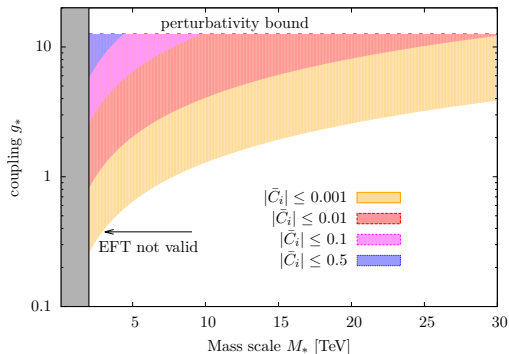


Figure : Areas in the $g_* - M_*$ plane. Coloured areas constrained in perturbative models subject to condition $C/\Lambda^2 = g_*^2/M_*^2$. Shaded grey area: mass scales $M_* < m_{t\bar{t}}^{\max}$

Consequences on EFT Validity

- Strength of constraints \iff range of EFT validity
- Match $\frac{C_i}{\Lambda^2} = \frac{g_*^2}{M_*^2}$
- Impose $M_* > m_{t\bar{t}}^{\max} = 2\text{TeV}$
- Weak constraint \implies larger g_* , higher-order corrections to BSM important
- Truncation at e.g. $\mathcal{O}(\Lambda^{-2})$ less reliable

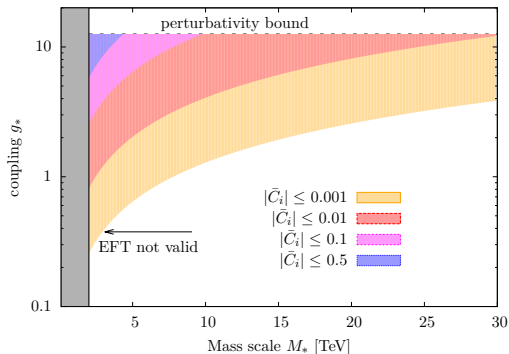


Figure : Areas in the $g_* - M_*$ plane. Coloured areas constrained in perturbative models subject to condition $C/\Lambda^2 = g_*^2/M_*^2$. Shaded grey area: mass scales $M_* < m_{t\bar{t}}^{\max}$

Consequences on EFT Validity

- Large $\bar{C}_i \gtrsim 0.5 \implies$
small area constrained,
large g_* likely to
invalidate tree-level
matching condition
- At 3 ab^{-1} , projected
constraints typically
 $\bar{C}_i \lesssim 0.01 \implies$ even
for moderate values of
 g_* , constraints
indirectly probe mass
scales much higher
than the kinematic
reach of the LHC

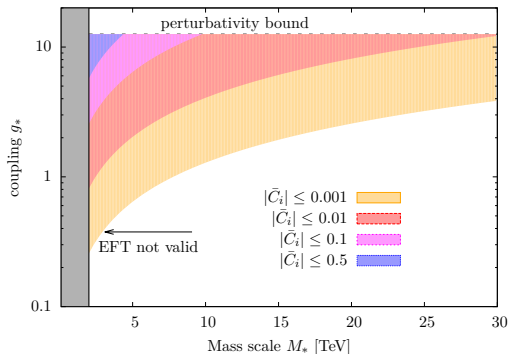


Figure : Areas in the $g_* - M_*$ plane. Coloured areas constrained in perturbative models subject to condition $C/\Lambda^2 = g_*^2/M_*^2$. Shaded grey area: mass scales $M_* < m_{t\bar{t}}^{\max}$

Consequences on EFT Validity

- Large $\bar{C}_i \gtrsim 0.5 \implies$ small area constrained, large g_* likely to invalidate tree-level matching condition
- At 3 ab^{-1} , projected constraints typically $\bar{C}_i \lesssim 0.01 \implies$ even for moderate values of g_* , constraints indirectly probe mass scales much higher than the kinematic reach of the LHC

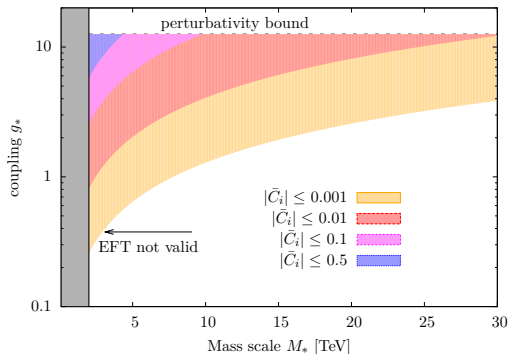


Figure : Areas in the $g_* - M_*$ plane. Coloured areas constrained in perturbative models subject to condition $C/\Lambda^2 = g_*^2/M_*^2$. Shaded grey area: mass scales $M_* < m_{t\bar{t}}^{\max}$



Summary

- A question that remains after the first results from LHC Run I is **how far EFT constraints will improve with higher statistics and larger kinematic coverage**
- For representative experimental scenarios we performed a dedicated analysis for events with transverse momenta $p_T^t \geq 200$ GeV where top-tagging becomes relevant
- We investigated the **relative improvements to constraints on the leading dimension-six operators** in top pair production
- Despite the efficient top reconstruction offered by jet substructure algorithms in the sensitive region of phase space, **combined limits from boosted and resolved events offer overall only marginal improvements**

Summary

- A question that remains after the first results from LHC Run I is **how far EFT constraints will improve with higher statistics and larger kinematic coverage**
- For representative experimental scenarios we performed a **dedicated analysis for events with transverse momenta $p_T^t \geq 200$ GeV where top-tagging becomes relevant**
- We investigated the **relative improvements to constraints on the leading dimension-six operators** in top pair production
- Despite the efficient top reconstruction offered by jet substructure algorithms in the sensitive region of phase space, **combined limits from boosted and resolved events offer overall only marginal improvements**

Summary

- A question that remains after the first results from LHC Run I is **how far EFT constraints will improve with higher statistics and larger kinematic coverage**
- For representative experimental scenarios we performed a **dedicated analysis for events with transverse momenta $p_T^t \geq 200$ GeV where top-tagging becomes relevant**
- We investigated the **relative improvements to constraints on the leading dimension-six operators** in top pair production
- Despite the efficient top reconstruction offered by jet substructure algorithms in the sensitive region of phase space, **combined limits from boosted and resolved events offer overall only marginal improvements**

Summary

- A question that remains after the first results from LHC Run I is **how far EFT constraints will improve with higher statistics and larger kinematic coverage**
- For representative experimental scenarios we performed a **dedicated analysis for events with transverse momenta $p_T^t \geq 200$ GeV where top-tagging becomes relevant**
- We investigated the **relative improvements to constraints on the leading dimension-six operators** in top pair production
- Despite the efficient top reconstruction offered by jet substructure algorithms in the sensitive region of phase space, **combined limits from boosted and resolved events offer overall only marginal improvements**

Conclusions

- The **boosted selection is generally saturated by large statistical uncertainties** for the expected \mathcal{L}_{int} of Run II, rendering improvements to systematics less important relative to the resolved selection
- Boosted top quarks from $t\bar{t}$ production are **sensitive to NP-induced modified gluon self-couplings through \mathcal{O}_G** . The remaining operators' weaker scaling with p_T leads to relatively looser bounds.
- For a **resolved analysis** targeting tops w/ $p_T^t \lesssim 200\text{GeV}$, sensitivity to NP-induced deviations is more of a trade-off between weaker distinguishability from the SM and more plentiful data, with **higher statistics and improved systematics offering comparable benefits**
- Theoretical uncertainties are not the limiting factors for the foreseeable future, but will become relevant at very large \mathcal{L}_{int}

Conclusions

- The **boosted selection is generally saturated by large statistical uncertainties** for the expected \mathcal{L}_{int} of Run II, rendering improvements to systematics less important relative to the resolved selection
- Boosted top quarks from $t\bar{t}$ production are **sensitive to NP-induced modified gluon self-couplings through Q_G** . The remaining operators' weaker scaling with p_T leads to relatively looser bounds.
- For a **resolved analysis** targeting tops w/ $p_T^t \lesssim 200\text{GeV}$, sensitivity to NP-induced deviations is more of a trade-off between weaker distinguishability from the SM and more plentiful data, with **higher statistics and improved systematics offering comparable benefits**
- Theoretical uncertainties are not the limiting factors for the foreseeable future, but will become relevant at very large \mathcal{L}_{int}

Conclusions

- The **boosted selection is generally saturated by large statistical uncertainties** for the expected \mathcal{L}_{int} of Run II, rendering improvements to systematics less important relative to the resolved selection
- Boosted top quarks from $t\bar{t}$ production are **sensitive to NP-induced modified gluon self-couplings through Q_G** . The remaining operators' weaker scaling with p_T leads to relatively looser bounds.
- For a **resolved analysis** targeting tops w/ $p_T^t \lesssim 200\text{GeV}$, sensitivity to NP-induced deviations is more of a trade-off between weaker distinguishability from the SM and more plentiful data, with **higher statistics and improved systematics offering comparable benefits**
- Theoretical uncertainties are not the limiting factors for the foreseeable future, but will become relevant at very large \mathcal{L}_{int}

Conclusions

- The **boosted selection is generally saturated by large statistical uncertainties** for the expected \mathcal{L}_{int} of Run II, rendering improvements to systematics less important relative to the resolved selection
- Boosted top quarks from $t\bar{t}$ production are **sensitive to NP-induced modified gluon self-couplings through \mathcal{O}_G** . The remaining operators' weaker scaling with p_T leads to relatively looser bounds.
- For a **resolved analysis** targeting tops w/ $p_T^t \lesssim 200\text{GeV}$, sensitivity to NP-induced deviations is more of a trade-off between weaker distinguishability from the SM and more plentiful data, with **higher statistics and improved systematics offering comparable benefits**
- Theoretical uncertainties are not the limiting factors for the foreseeable future, but will become relevant at very large \mathcal{L}_{int}

Backup - HEPTopTAgger

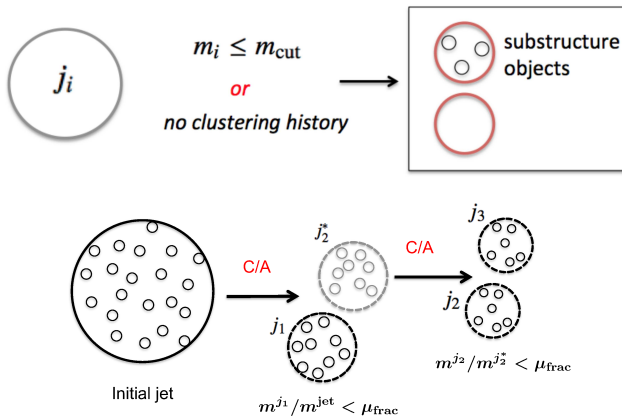


Figure : HEPTopTAgger Illustration - Image: (Aad et al. 1306.4945)

Backup - HEPTopTAgGER

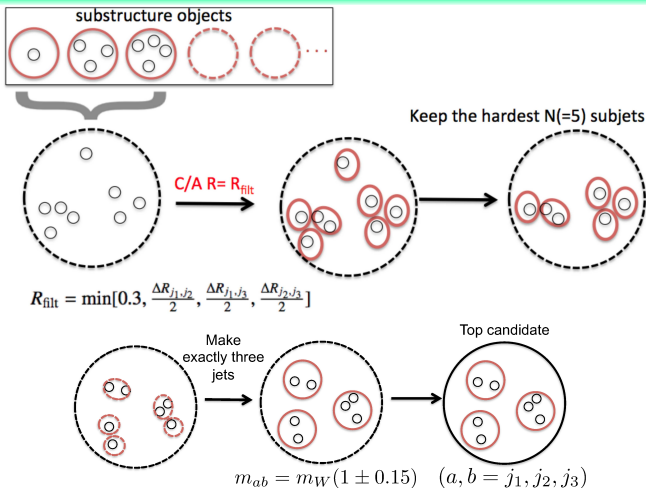


Figure : HEPTopTAgGER Illustration - Image: [\(Aad et al. 1306.4945\)](#)